Proc. Int. Workshop on Nitride Semiconductors
IPAP Conf. Series 1 pp. 661-664

Overdamped Electron Plasma Oscillations in Cubic $Al_xGa_{1-x}N$ Layers Observed by Raman Scattering Spectroscopy

J.R.L. FERNANDEZ[1*], A. TABATA[1], V.A. CHITTA[1], D.J. AS[2], T. FREY[2], O.C. NORIEGA[1], M.T.O. SILVA[1], E. ABRAMOF[3], D. SCHIKORA[2], K. LISCHKA[2], and J.R. LEITE[1]

[1] *Instituto de Física, Universidade de São Paulo, CP66318, 05315-970 São Paulo, SP, Brazil*
[2] *Universität Paderborn, FB-6 Physik, D-33095 Paderborn, Germany*
[3] *Instituto Nacional de Pesquisas Espaciais (INPE-LAS), CP 515, 12201-970 São José dos Campos, SP, Brazil*

Longitudinal-optic (LO) phonon-plasmon coupled modes in n-type cubic (c-)$Al_xGa_{1-x}N$/GaN epitaxial layers are investigated by Raman scattering measurements. The samples were grown by molecular beam epitaxy on GaAs(001) substrates using a radio-frequency plasma nitrogen source. The nominally undoped layers show high electron concentrations ($n \cong 10^{20} cm^{-3}$), displaying a metallic behavior in the range of temperature from 15 to 300K. The high electron concentrations and low electron mobilities in our samples are such that the c-$Al_xGa_{1-x}N$ layers are overdamped plasma systems which are confirmed by line shape analysis of the measured Raman spectra.

KEYWORDS: Raman spectroscopy, cubic AlGaN, GaN, molecular beam epitaxy, Hall-effect, phonon-plasmon coupling

1. Introduction

Nanostructures based on the group-III nitride semiconductors have been extensively used in the past few years in the fabrication of optoelectronic devices operating in the green-blue-UV region of the spectrum[1]. As wide band-gap materials, they also have been succesfully used to fabricate high voltage, high temperature, and high frequency electronic devices.[2-4] Although almost all the applications made so far are based on the hexagonal (h-) phase of the materials, recently cubic (c-)GaN layers grown on GaAs(001) substrates have been used to make p-n junction light emitting diodes.[5,6] It is well established now that the growth of cubic nitride-based layers and the investigation of their properties are highly desirable under both, basic and applied points of view.[7] In the present work free-carrier gas systems are investigated in n-type c-$Al_xGa_{1-x}N$/GaN epitaxial layers. The Raman scattering technique is used to observe longitudinal-optic (LO)-phonon-plasmon coupled modes originated from the high-concentration electron gas present in the non intentionally doped samples.[8]

The magnitude of plasmon damping observed by Raman scattering in n-type h-GaN and c-GaN has been subject of recent discussion in the literature.[9-12] For high electron concentrations (10^{18}-$10^{19} cm^{-3}$) and low electron mobilities, the plasmon damping constant Γ is expected to be larger than the plasma frequency ω_p and the electron gas behaves as an overdamped plasma system. The observation of this regime has been reported for h- and c-GaN epitaxial layers.[10,12] For relatively low concentration and high mobility of the electron carriers, the regime $\Gamma < \omega_p$ is reached and the free-electron gas behaves as an underdamped plasma system. Such behavior has been observed in high quality n-type h-GaN epitaxial layers with carrier densities in the range of 10^{17}-$10^{18} cm^{-3}$.[9]

Hall-effect measurements carried out by us for the c-$Al_xGa_{1-x}N$ layers lead to electron concentrations in the range of 10^{20} to $10^{21} cm^{-3}$. The observed electron mobilities are lower than about $20 cm^2/Vs$. As a consequence, a broad band covering a large region between the transverse-optic (TO) and LO phonon frequencies of the alloy is observed in the Raman spectra of the layers. A spectral line shape analysis shows that this band arises from overdamped plasmon-phonon scattering dominated by a charge-density-fluctuation (CDF) mechanism.

2. Sample Preparation

The c-$Al_xGa_{1-x}N$/GaN layers ($0.07<x<0.25$) were grown on GaAs(001) substrates by molecular beam epitaxy (MBE) using Al, Ga and As conventional solid source effusion cells and a radio-frequency plasma nitrogen source. The c-GaN buffer layers were grown at 720°C with a thickness of about 350nm. The c-AlGaN layers were grown at higher temperature of T=835°C. The growth rate of the AlGaN layers was about 80nm/h. The growth front was continuously monitored by reflection high electron diffraction (RHEED) and the diffraction patterns exhibit a cubic symmetry along all major azimuths. Rutherford Backscattering Spectroscopy (RBS) experiments were carried out for an accurate determination of the alloy composition in the films[13] and high resolution X-ray diffraction (HRXD) measurements were made to monitor the cubic structure and crystalline quality of the c-$Al_xGa_{1-x}N$/GaN layers. Details of the growth procedure and structural analysis of the samples are being reported on Ref. 14.

3. Electrical Measurements

The resistivity of the c-$Al_xGa_{1-x}N$/GaN layers as a function of inverse temperature is shown in Fig. 1. The nominally undoped samples show metallic behavior in the range of temperature from 15 to 300K. The Hall carrier concentration n and mobility μ as a function of temperature for the layers were also measured and the obtained results at 300K are shown in Table I. The Hall-effect measurements were made with the standard square shaped samples van der Pauw geometry. It has been shown that c-GaN and c-InN can be easily grown as n-type layers.[15,16] At the beginning, N vacancies were associated to this property, however, there is a consensus now that the O replacing N should be the active shallow

*E-mail address: rafael@macbeth.if.usp.br

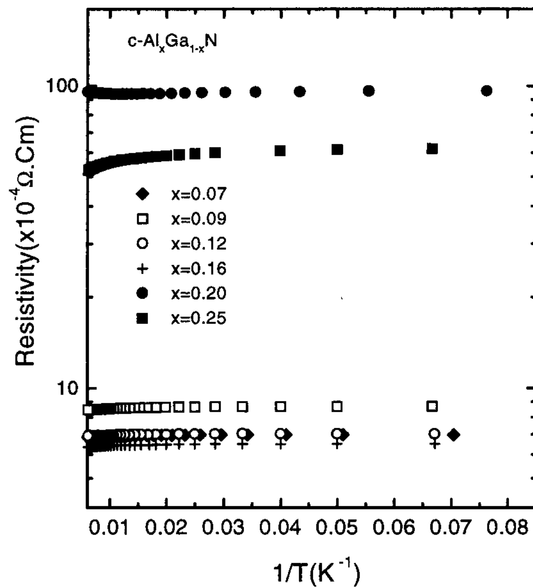

Fig. 1. Resistivity as a function of inverse temperature for the c-$Al_xGa_{1-x}N$ layers. The alloy composition of each sample is indicated.

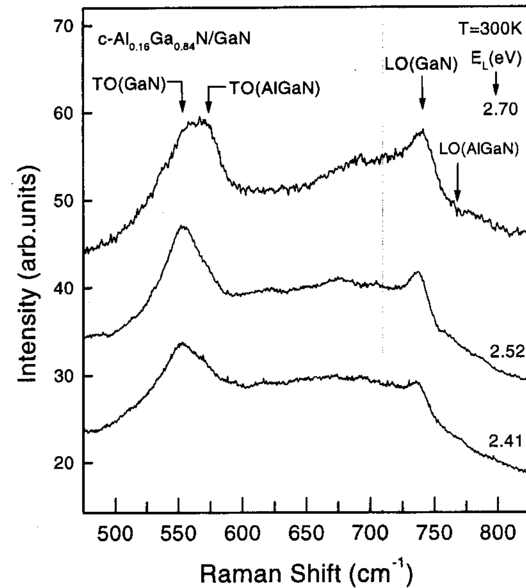

Fig. 2. Room temperature micro-Raman spectra of the c-$Al_{0.16}Ga_{0.84}N$/GaN sample recorded for three different excitation energies E_L.

Table I – Electron concentration, n, mobility μ and TO phonon frequency at Γ for the c-$Al_xGa_{1-x}N$/GaN layers.

x	n($10^{20}cm^{-3}$)	μ(cm^2/Vs)	TO(cm^{-1})
0.07	4.12	21.76	559
0.09	3.44	21.35	560
0.12	6.06	14.82	564
0.16	6.20	15.89	567
0.20	1.32	5.50	569
0.25	26.4	0.52	570

donor in these materials. O is related to the strong n-type doping observed in nominally undoped h-AlGaN alloys.[2] Probably O is also related to the origin of the high-doping level found in our samples. Although there have been several reports on the behavior of O in h-AlGaN, no such studies exist so far for the cubic modification of the alloy. These investigations are highly desirable.

4. Micro-Raman Spectra

The micro-Raman experiments were carried out at room temperature using a T64000 Jobin-Yvon Raman system with a charge coupled device as a detector. The 2.41, 2.52 and 2.70eV lines from an argon-ion laser are employed as the excitation and the power was kept below 3mW. The microscope objective in the apparatus allows the laser beam to be focused on a spot of about 2μm. The measurements were carried out in backscattering from (001) surface. The incident radiation is polarized along the [110] crystallographic direction and no analyser is used in the scattered light path.

Fig.2 shows the micro-Raman spectra of the c-$Al_{0.16}Ga_{0.84}N$/GaN layer recorded for three different excitation energies. Similar results were obtained for the other samples. The c-GaN phonon frequencies 555cm^{-1} (TO) and 741cm^{-1} (LO) are clearly identified in the spectra.[17] We were able to identify for all analysed layers the TO phonon frequency of the alloy as indicated in the Figure. Assuming Lorentzian line shapes the observed TO peaks for the alloys were fitted after background subtraction and their frequencies were determined and listed in Table I. A good agreement is found between the values of the TO frequencies obtained by us and those recently determined by Raman measurements on c-$Al_xGa_{1-x}N$ layers grown by MBE on c-SiC/Si substrates.[18] The LO phonon frequency of the alloy does not appear in our spectra. The indication made in Fig. 2 refers to the result reported in Ref. 18. By focusing the laser beam at different spots on the sample, we observe that the broad band appearing in the central part of the spectra changes its relative intensity and width. Micro-Raman is probing the spatial distribution of electron concentration in the layers through the charge density dependent LO phonon-plasmon coupled modes.[9]

5. Line Shape Analysis

In this section we perform the simulation of the Raman spectra of the c-$Al_xGa_{1-x}N$ layers by adopting a theoretical approach suitable to describe the overdamped plasma excitations within the framework of the CDF mechanism.[8,12] We show the results of our analysis for the sample $Al_{0.2}Ga_{0.8}N$/GaN layer. We start by comparing the values of $\Gamma=e/\mu m^*$ and $\omega_p=(e^2n/\varepsilon_o\varepsilon(\infty)m^*)^{1/2}$ for this sample. The values 0.15-0.22 were reported for the electron effective mass m^* in c-GaN, in units of electron rest mass.[19] For the c-AlN compound the value m^* is reported as 0.19.[20] We use the value m^*=0.20 for the calculation of Γ and ω_p for the alloy. The values $\varepsilon(\infty)$=5.0 and 4.68 have been reported for the dielectric constants of c-GaN and h-AlN, respectively.[19,21] The value 4.8 was adopted by us for $\varepsilon(\infty)$ of the alloy, leading to the results

Γ=8.5x10^{3}cm^{-1} and ω_p=3.3x10^{3}cm^{-1} for the c-$Al_{0.2}Ga_{0.8}N$/GaN sample. Thus, we expect that the main features observed in the Raman spectra of the c-$Al_{0.2}Ga_{0.8}N$ layer should be simulated by assuming it as an overdamped plasma system.

The total dielectric function of the coupled plasmon-optical phonons is given by

$$\varepsilon(q,\omega) = \varepsilon(\infty) + \chi_L(\omega) + \chi(q,\omega) \quad , \tag{1}$$

$$\chi_L(\omega) = \varepsilon(\infty)\frac{\omega_{LO}^2 - \omega_{TO}^2}{\omega_{TO}^2 - \omega^2 - i\omega\gamma} \ , \tag{2}$$

$$\chi(q,\omega) = \frac{(1+\frac{i\Gamma}{\omega})\chi^o(q,\omega+i\Gamma)}{1+(\frac{i\Gamma}{\omega})\frac{\chi^o(q,\omega+i\Gamma)}{\chi^o(q,0)}} \ , \tag{3}$$

where $\chi_L(\omega)$ and $\chi(q,\omega)$ are the phonon and electron dielectric functions, respectively. The $\chi(q,\omega)$ was calculated using the Lindhard-Mermin expression where $\chi^o(q,\omega)$ is the Lindhard expression for a parabolic conduction band and T=0. [22,23]

$$\chi^o(q,\omega) = \frac{3\omega_p^2}{(qV_F)^2}[\frac{1}{2}+\frac{1}{8z}\{1-(z-u)^2\}\ln(\frac{z-u+1}{z-u-1})$$
$$+\frac{1}{8z}\{1-(z+u)^2\}\ln(\frac{z+u+1}{z+u-1})] \ , \tag{4}$$
$$z = \frac{q}{2k_F} \ ,$$
$$u = \frac{\omega+i\Gamma}{qV_F} \ ,$$

where k_F, V_F and γ are the Fermi wavevector , Fermi velocity, and phonon damping constant.

To calculate the Raman spectrum we integrate the response function, $L(q,\omega)$, with a weight $F(q)$ from zero to q_{max}, which corresponds to the decrease in the electron-phonon coupling with increasing q.

$$I(\omega) = \int_0^{q_{max}} L(q,\omega)F(q)dq \ . \tag{5}$$

In our case we assume the CDF scattering mechanism,

$$L(q,\omega) = q^2(1-e^{-\hbar\omega/K_BT})^{-1}\left(\frac{\omega_{LO}^2-\omega^2}{\omega_{TO}^2-\omega^2}\right)\mathrm{Im}(\frac{-1}{\varepsilon(q,\omega)}) \ , \tag{6}$$

$$F(q) = (\frac{4\Pi}{q^2+q_{FT}^2})^2 \ . \tag{7}$$

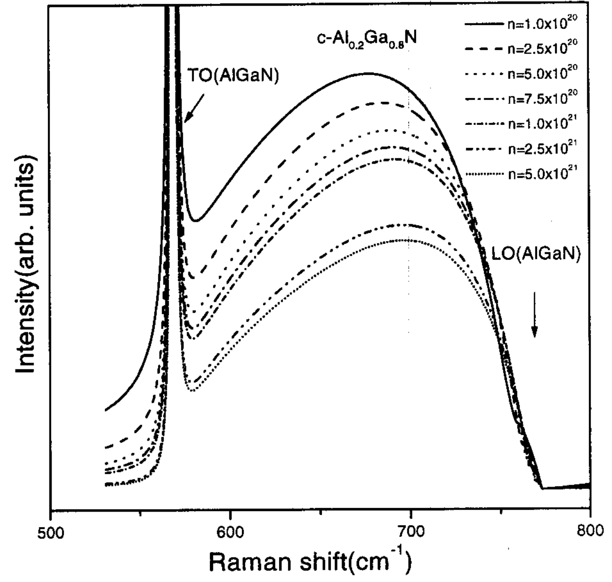

Fig 3. Line shape simulation of the Raman spectra for the c-$Al_{0.2}Ga_{0.8}N$ alloy. Different values of electron concentration (cm^{-3})were considered in the calculations.

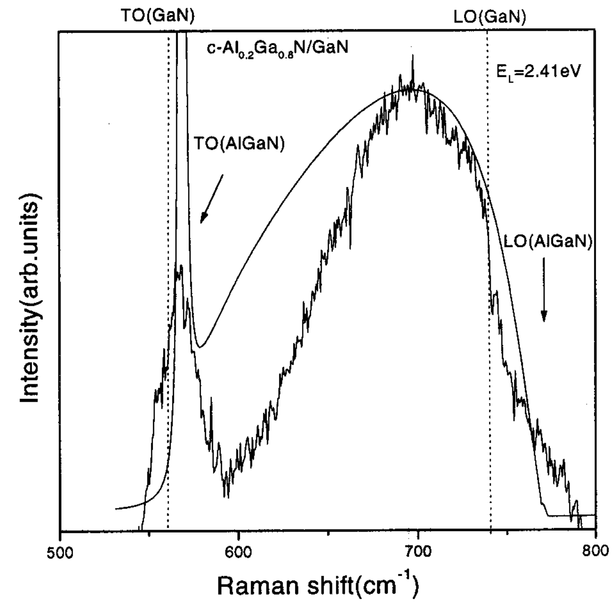

Fig. 4. Micro-Raman spectrum of the c-$Al_{0.2}Ga_{0.8}N$/GaN layer recorded for E_L=2.41eV. The smooth solid line is the theoretical simulation of the spectrum. The dashed lines denote the TO and LO frequencies of c-GaN.

We adopt a Fourier transform of a Yukawa potential due to the high electron concentration in the layer. The F(q) term takes into account q nonconservation mechanism. In Eq.(7), q_{FT} is the Fermi-Thomas screening wave vector.

The Raman spectra of the $Al_{0.2}Ga_{0.8}N$ alloy layer simulated according to Eq.(5) is show in Fig. 3 for several values of the carrier concentration in a high level doping regime. The values of the parameters m^*, $\varepsilon(\infty)$, Γ and TO frequency used to calculate $I(\omega)$ for this layer are already given in the text. For the alloy LO frequency, we took the value 770cm^{-1} according to Ref.18 and the phonon damping constant γ was taken as 0.01cm^{-1}. The cutoff wave vector q_{max}=5.0 q_{FT} was assumed as the superior

limit of the integral in Eq.(5). No significant changes in the line shapes occur if larger values of q_{max} are used. As observed in our experiments, the calculated Raman spectra are dominated by a broad band lying between the alloy TO and LO frequencies. The comparison between the room temperature micro-Raman spectrum recorded at E_L=2.41eV for the c-$Al_{0.2}Ga_{0.8}N$/GaN layer with the result of the theoretical simulation is madê in Fig. 4. The line shape was calculated assuming $n=2.5x10^{21}cm^{-3}$ which is much higher than the measured value listed in Table I. However, we have to take into account the fact that Hall-effect measurement leads to an averaged value for the concentration while micro-Raman is probing a small region of the sample where the concentration can be higher.

6. Conclusions

Cubic $Al_xGa_{1-x}N$/GaN layers ($0.07<x<0.25$) grown by MBE on GaAs(001) substrates were investigated by micro-Raman scattering. The TO frequencies at Γ for the alloy were determined and a good agreement with the TO phonon mode frequencies previously reported was found. The LO phonon mode of the alloy was not identified in the spectra. In our analysis of the data, we assume for the frequency of the LO mode values recently reported in the literature. The main feature of all the observed micro-Raman spectra is the presence of a broad band covering a large region between the TO and LO phonon frequencies of the alloy. We interpret this band as originated from LO phonon-plasmon coupling from an overdamped high-concentration free-electron gas plasma present in our layers.

Theoretical line shape simulations of the Raman spectra of the c-$Al_xGa_{1-x}N$ alloys were performed by assuming that the charge-density-fluctuation is the dominant mechanism in the scattering process. The calculated line shapes of the alloys Raman spectra are quite similar to the line shapes of the spectra taken from our samples. The best agreement between theory and experiment is reached when the spectra are recorded using the lower excitation energy E_L=2.41eV. For excitation energy E_L=2.70eV, which is closer to the alloy band gap, the impurity-induced Fröhlich mechanism plays a hole and the calculated line shapes start to deviate from those observed from experiment. Recent Raman scattering data have shown that the c-$Al_xGa_{1-x}N$ alloy is a two (one) phonon mode system for TO(LO).[18] The AlN-related TO phonon frequency reported (≅650cm^{-1}) lies just in the region where the broad bands arise in our experiments. We do not detect the AlN-related TO phonon modes of the alloy in the micro-Raman spectra of our layers. In our line shape analysis we are taking into account only the TO mode observed by us in the Raman spectra.

Acknowledgments

This work was performed with support from CNPq, CAPES and FAPESP (Brazilian funding agencies) and DFG (Deutsche Forschungsgemeinschaft).

1) S. Nakamura and G. Fasol: *The Blue Laser Diode* (Springer, Berlin, 1997).
2) B. Monemar: J. Mater. Sci. **10** (1999) 227.
3) S.J. Pearton, J.C. Zolper, R.J. Shul and F. Ren: J. Appl. Phys. **86** (1999) 1.
4) J.W. Orton and C.T. Foxon: Rep. Prog. Phys. **61** (1998) 1.
5) H. Yang, L.X. Zheng, J.B. Li, X.J. Wang, D.P. Xu, Y.T. Wang, X.W. Hu and P.D. Han: Appl. Phys. Lett. **74** (1999) 2498.
6) D.J. As, A. Richter, J. Busch, M. Lübbers, J. Mimkes and K. Lischka: Appl. Phys. Lett. **76** (2000) 13.
7) S.F. Chichibu, A.C. Abare, M.P. Mack, M.S. Minsky, T. Deguchi, D. Cohen, P. Kozodoy, S.B. Fleischer, S. Keller, J.S. Speck, J.E. Bowers, E. Hu, U.K. Mishra, L.A. Coldren, S.P. DenBaars, K. Wada, T. Sota and S. Nakamura: Mater. Sci. Engineer. **B59** (1999) 298.
8) G. Abstreiter, M. Cardona and A. Pinczuk: *Light Scattering in Solids IV*, edited by M. Cardona and G. Güntherodt (Springer, Berlin, 1984) p.5.
9) H. Harima, H. Sakashita and S. Nakashima: Mater. Sci. Forum **264-268** (1998) 264.
10) T. Kozawa, T. Kachi, H. Kano, Y. Taga, M. Hashimoto, N. Koide and K. Manabe: J. Appl. Phys. **75** (1994) 1098.
11) P. Perlin, J. Camassel, W. Knap, T. Taliercio, J.C. Chervin, T. Suski, I. Grzegory and S. Porowski: Appl. Phys. Lett. **67** (1995) 2524.
12) M. Ramsteiner, O. Brandt and K.H. Ploog: Phys. Rev. **B58** (1998) 1118.
13) J. Portmann, C. Haug, R. Brenn, T. Frey, B. Schöttker, D.J. As: Nucl. Inst. and Meth. **B155** (1999) 489.
14) T. Frey, D.J. As, M. Bartels, A. Pawlis, K. Lischka, A. Tabata, J.R.L. Fernandez, J.R. Leite, C. Haug and R. Brenn: To be published.
15) D.J. As, D. Schikora, A. Greiner, M. Lübbers, J. Mimkes and K. Lischka: Phys. Rev. **B54** (1996) R11118.
16) J.R.L. Fernandez, A. Tabata, J.R. Leite, A.P. Lima, V.A. Chitta, E. Abramof, D.J. As, D. Schikora and K. Lischka: MRS Internet J. Nitride Semicond. Res. **5S1** (2000) W3.40.
17) A. Tabata, R. Enderlein, J.R. Leite, S.W. da Silva, J.C. Galzerani, D. Schikora, M. Kloidt and K. Lischka: J. Appl. Phys. **79** (1996) 4137.
18) H. Harima, T. Inoue, S. Nakashima, H. Okumura, Y. Ishida, S. Yoshida, T. Koizumi, H. Grille and F. Bechstedt: Appl. Phys. Lett. **74** (1999) 191.
19) S.A. McGill, K. Cao, W.B. Fowler and G.G. DeLeo: Phys. Rev. **B57** (1998) 8951.
20) S.K. Pugh, D.J. Dugdale, S. Brand, R.A. Abram: Semicond. Sci. Technol. **14** (1999) 23.
21) H. Morkoç: *Nitride Semiconductor and Devices* (Springer, Berlin, 1999).
22) J. Lindhard: Dan. Mat. Medd. **28** (1954).
23) N.D. Mermin: Phys. Rev. **B1** (1970) 2362.

View publication stats